

Immobilizing Au Nanoparticles with Polymer Single Crystals, Patterning and Asymmetric Functionalization

Bing Li and Christopher Y. Li*

A. J. Drexel Nanotechnology Institute and Department of Materials Science and Engineering, Drexel University, Philadelphia, Pennsylvania 19104

Received September 25, 2006; Revised Manuscript Received November 30, 2006; E-mail: chrisli@drexel.edu

Considerable attention has been paid to nanoparticle (NP) research due to their fascinating properties and potential applications in nanotechnology and biotechnology.¹ Achieving ordered NP arrays is one of the major research goals in the field.^{1,2} A number of different methods have been used to fabricate ordered NP structures, including crystallization of functionalized NPs,^{1,3} self-assembly of NPs at the liquid–liquid interface,⁴ block copolymer templating,⁵ etc. Asymmetrically functionalizing NPs is of particular interest since it could directly lead to controlled patterning of NPs into complex structures for a variety of applications.^{6,7} Via computer simulation, Glotzer et al. proposed a variety of possible assembly routes for asymmetrically functionalized NPs (or patchy particles).⁷ Experimentally, in the colloid science community, numerous techniques have been developed to synthesize patchy particles with relatively large size.⁸ However, it still remains a challenging task to achieve asymmetrically functionalized NPs with small diameters (<20 nm). To this end, an elegant approach of using DNA to functionalize gold NPs (AuNPs) has been investigated by a few research groups, and asymmetric NP functionalization has been achieved.⁹ Synthesis of monolayer-protected AuNPs with a single surface functional group has also been reported using a solid phase synthesis technique.¹⁰ Anisotropic deposition of AuNPs on organic single crystals was also recently reported.¹¹ Most of these methods either used a kinetic control approach or employed a solid phase substrate to achieve asymmetric NP functionalization.

In this communication, we report, for the first time, using polymer lamellar single crystals as the solid substrate to create a patterned functional (thiol) surface and to immobilize AuNPs. We demonstrated that patterning of AuNPs could be achieved, and the AuNP area density could be easily controlled by polymer molecular weight (MW). Furthermore, this unique technique also enables asymmetric functionalization of AuNPs. In one example, bilayer AuNP/polymer hybrids were obtained. Subsequent dissolution of the hybrids led to free asymmetric binary AuNP complexes.

In our preliminary work, thiol-terminated polyethylene oxide (HS-PEO) was used as the model polymer since (1) AuNPs can be functionalized with HS-PEO using the “graft-to” method;¹² (2) solution crystallization of PEO has been extensively investigated, and large, uniform single crystals can be easily achieved.¹³ The detailed experimental procedure can be found in Supporting Information. The number-average molecular weights of PEO were 2K and 48.5K g/mol, respectively. As long chain polymers crystallize from solution or melt, they fold back and forth forming quasi-two-dimensional lamellae with a typical thickness of 5–20 nm. In the present case, large size, square-shaped lamellar single crystals were obtained using the self-seeding method, and a transmission electron microscopy (TEM) image of such single crystals is shown in Figure S1. Most of the thiol groups (or some of them, depending on MW; see following discussion) were excluded onto the crystal surface upon crystallization, as shown in

Scheme 1. Immobilizing AuNPs on HS-PEO Single Crystals

Scheme 1b. These HS-PEO single crystals were incubated with tetraoctylammonium bromide (TOAB)-protected AuNPs (~5 nm in diameter) for ~2 h, and AuNPs were then immobilized onto the single crystal surface due to the Au–S bond formation (Scheme 1c).

Figure 1a shows the TEM images of AuNPs on the HS-PEO (48.5K) single crystal (inset shows the entire single crystal). AuNPs can be clearly seen on the surface as the dark dots. The AuNP area density is relatively low, and the NPs are randomly located. Much denser arrangement of AuNPs can be seen in the case of the 2K HS-PEO, as shown in Figure 1b, where most of the single crystal surface was covered with AuNPs. The inset shows a 6 × 6 μm, square-shaped AuNP monolayer, and the size can be easily controlled by crystallization time. The difference of the AuNP area density on 2K and 48.5K PEO crystals can be attributed to the different thiol group density on the PEO single crystal surface as shown in Figure 1c,d. For 48.5K PEO, the polymer chain end density is much lower than that of 2K PEO (~24 times less, assuming similar lamellar thickness). Furthermore, low MW PEO undergoes integral folding, which renders most of the chain ends on the crystal surface, while for relatively long chain PEO, nonintegral folding occurs.^{13,14} In this case, despite the fact that thiol groups are different from the rest of the polymer chain, they could be embedded in the lamellar crystals, as shown in Figure 1c. This further reduces the thiol population on the 48.5K crystal surface. Therefore, PEO MW can be used as a controlling factor to tune the thiol (and thus AuNP) density on the PEO crystal

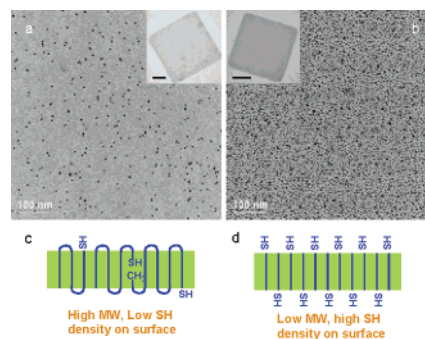


Figure 1. AuNPs on the surface of HS-PEO (a) 48.5K and (b) 2K single crystals (inset shows the entire single crystal, scale bar 2 μm). Schematic representation shows low thiol density on 48.5K PEO single crystal (c) and relatively high thiol density on 2K PEO single crystals (d). Note that extended chain single crystals are shown in d; folding could occur depending on MW and crystallization conditions.

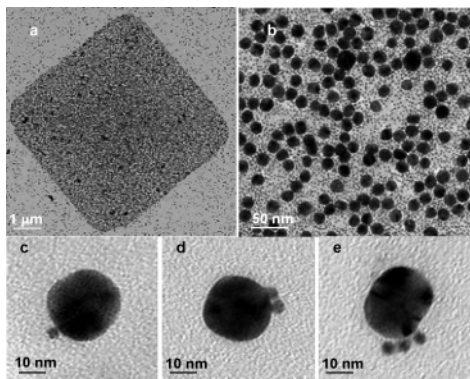
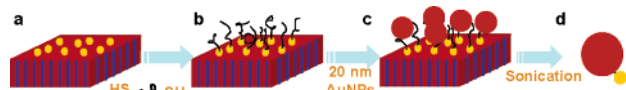


Figure 2. TEM micrographs of PEO single crystal templated AuNP bilayer (a, b) and binary AuNPs (c, e).

Scheme 2. Formation Mechanism of Bilayer AuNP/PEO Hybrids and Binary Nanoparticles



surface. A control experiment using 2K PEO with no thiol chain end (HO terminated) was also conducted. Similar single crystal structure was formed using solution crystallization. However, after the same incubation procedure, few AuNPs were observed on the HO-PEO crystal surface (Figure S2), which confirms that formation of the Au–S bond led to immobilization of AuNPs on the HS-PEO single crystal surface. It further suggests that, besides MW, we might potentially be able to use the HS-PEO and HO-PEO mixture to form the single crystals with controlled surface functional group density.

Due to the planar geometry of PEO single crystals, after the coupling reaction, as shown in Scheme 1, the bottom part of the AuNPs is functionalized with PEO while the top part is covered with TOAB. Asymmetrically functionalized AuNPs were thus achieved. Note that TOAB can be easily replaced with a variety of functional groups, and this provides a generic means to synthesize asymmetrically functionalized NPs. As a proof-of-concept, we applied hexanedithiol to functionalize the top portion of the AuNPs in Figure 1b. A second coupling reaction with larger AuNPs (20 nm) was then carried out, as shown in Scheme 2. AuNP bilayers were then formed on the PEO single crystal surface (Figure 2a). It can be clearly seen that the square-shaped PEO single crystals were covered by 20 nm AuNPs. Figure 2b shows the enlarged area of Figure 2a. AuNPs with different sizes can be seen on the PEO single crystal surface forming a bilayer structure. Note that the coverage of the second AuNP layer can be controlled by incubation time. The solid PEO single crystal substrate can also be easily dissolved, which allowed us to obtain free binary AuNPs. To this end, the bilayer AuNP/PEO hybrids were sonicated in ethanol for 0.5 h, and we anticipated to observe snowman-shaped binary AuNPs, as shown in Scheme 2d. Figure 2c–e shows the TEM images of the resulting NPs. Binary particles with two sizes can be clearly seen from Figure 2c. Interestingly, large AuNPs with 2 (or 3) small AuNPs attached could also be observed. This observation is not surprising since one 20 nm AuNP was accessible to multiple 5 nm AuNPs during the second incubation process, as shown in Figure 2b; bonding with hexanedithiol thus led to multiparticle complex, as shown in Figure 2d,e. UV–vis spectroscopy shows that the

surface plasmon band of the 20 nm AuNPs red shifts from 520 to 537 nm upon forming the complexes (Figure S3). Note that, for all these binary AuNP complexes in Figure 2c–e, 5 nm AuNPs stay only on a small part of the 20 nm AuNPs, and asymmetric functionalization could thus be confirmed. Similar AuNP complexes were also obtained by mixing free asymmetrically (PEO/hexanedithiol) functionalized 20 nm AuNPs with 5 nm AuNPs in solution, which further confirmed asymmetric functionalization of the AuNPs (Figure S4).

In summary, for the first time, AuNPs were immobilized on square-shaped PEO single crystals. The AuNP area density depends on the polymer MW. Due to the planar geometry of the single crystals, the AuNPs were also asymmetrically functionalized. Binary AuNP complexes were successfully obtained by dissolving the PEO single crystal substrate. This approach provides a novel means to pattern AuNPs and to synthesize asymmetrically functionalized AuNPs. We also anticipate that this methodology could be applied to other metallic or semiconducting NPs.

Acknowledgment. This work was supported by the NSF CAREER award (DMR-0239415), 3M, and DuPont.

Supporting Information Available: Experimental details, TEM images of polymer single crystals and AuNP complexes, and UV–vis spectra of AuNP complexes. This material is available free of charge via the Internet at <http://pubs.acs.org>.

References

- (1) (a) Murray, C. B.; Kagan, C. R.; Bawendi, M. G. *Annu. Rev. Mater. Sci.* **2000**, *30*, 545–610. (b) El-Sayed, M. A. *Acc. Chem. Res.* **2001**, *34*, 257–264. (c) Daniel, M.-C.; Astruc, D. *Chem. Rev.* **2004**, *104*, 293–346. (d) Schmid, G.; Simon, U. *Chem. Commun.* **2005**, 697–710.
- (2) (a) Pileni, M. P. *J. Phys. Chem. B* **2001**, *105*, 3358–3371. (b) Taleb, A.; Petit, C. *J. Phys. Chem. B* **1998**, *102*, 2214–2220. (c) Fendler, J. H. *Chem. Mater.* **2001**, *13*, 3196–3210. (d) Taleb, A.; Silly, F. *Adv. Mater.* **2000**, *12*, 633–637.
- (3) (a) Collier, C. P.; Vossmeier, T. *Annu. Rev. Phys. Chem.* **1998**, *49*, 371–404. (b) Katz, E.; Willner, I. *Angew. Chem., Int. Ed.* **2004**, *43*, 6042–6108.
- (4) (a) Lin, Y.; Skaff, H.; Emrick, T.; Dinsmore, A. D.; Russell, T. P. *Science* **2003**, *299*, 226–229. (b) Binder, W. H. *Angew. Chem., Int. Ed.* **2005**, *44*, 5172–5175.
- (5) (a) Thompson, R. B.; Ginzburg, V. V.; Matsen, M. W.; Balazs, A. C. *Science* **2001**, *292*, 2469–2472. (b) Bockstaller, M. R.; Lapetnikov, Y.; Margel, S.; Thomas, E. L. *J. Am. Chem. Soc.* **2003**, *125*, 5276–5277. (c) Zhang, Q.; Xu, T.; Butterfield, D.; Misner, M. J.; Ryu, D. Y.; Emrick, T.; Russell, T. P. *Nano Lett.* **2005**, *5*, 357–361. (d) Chiu, J. J.; Kim, B. J.; Kramer, E. J.; Pine, D. J. *J. Am. Chem. Soc.* **2005**, *127*, 5036–5037.
- (6) de Gennes, P. G. *Croat. Chem. Acta* **1998**, *71*, 833–836.
- (7) (a) Zhang, Z. L.; Glotzer, S. C. *Nano Lett.* **2004**, *4*, 1407–1413. (b) Glotzer, S. C. *Science* **2004**, *306*, 419–420.
- (8) (a) Manoharan, V. N.; Elssesser, M. T.; Pine, D. J. *Science* **2003**, *301*, 483–487. (b) Lu, Y.; Yin, Y.; Xia, Y. *Adv. Mater.* **2001**, *13*, 415–420. (c) Shi, W.; Zeng, H.; Sahoo, Y.; Ohulchanskyy, T. Y.; Ding, Y.; Wang, Z. L.; Swihart, M.; Prasad, P. N. *Nano Lett.* **2006**, *6*, 875–881.
- (9) (a) Mirkin, C. A.; Letsinger, R. L.; Mucic, R. C.; Storhoff, J. J. *Nature* **1996**, *382*, 607–609. (b) Alivisatos, A. P.; Johnson, K. P.; Peng, X.; Wilson, T. E.; Loweth, C. J.; Bruchez, M. P., Jr.; Schultz, P. G. *Nature* **1996**, *382*, 609–611. (c) Loweth, C. J.; Caldwell, W. B.; Peng, X.; Alivisatos, A. P.; Schultz, P. G. *Angew. Chem., Int. Ed.* **1999**, *38*, 1808–1812. (d) Mbindyo, J. K. N.; Reiss, B. D.; Martin, B. R.; Keating, C. D.; Natan, M. J.; Mallouk, T. E. *Adv. Mater.* **2001**, *13*, 249–254. (e) Xu, X.; Rosi, N. L.; Wang, Y.; Huo, F.; Mirkin, C. A. *J. Am. Chem. Soc.* **2006**, *128*, 9286–9287.
- (10) (a) Sung, K. M.; Mosley, D. W.; Peelle, B. R.; Zhang, S.; Jacobson, J. M. *J. Am. Chem. Soc.* **2004**, *126*, 5064–5065. (b) Worden, J. G.; Shaffer, A. W.; Huo, Q. *Chem. Commun.* **2004**, 518–519.
- (11) Fujiki, Y.; Tokunaga, N.; Shinkai, S.; Sada, K. *Angew. Chem., Int. Ed.* **2006**, *45*, 4764–4767.
- (12) Wuelfing, W. P.; Gross, S. M. *J. Am. Chem. Soc.* **1998**, *120*, 12696–12697.
- (13) Kovacs, A. J.; Straupe, C. J. *Polym. Sci., Polym. Symp.* **1977**, *59*, 31–54.
- (14) Cheng, S. Z. D.; Chen, J. H.; Barley, J. S.; Zhang, A. Q.; Habenschuss, A.; Zschack, P. R. *Macromolecules* **1992**, *25*, 1453–1460.

JA0668318